International Journal of Mechatronics and Applied Mechanics
2025, Issue 20, Vol. 1

DESIGN OF NOMA SCHEME AND CHANNEL ESTIMATION IN INTELLIGENT SIGNAL PROCESSING

Li Zhang
School of Electrical and Electronic Engineering,
ZhengZhou Railway Vocational & Technical College
ZhengZhou, 450052, China
E-mail: 11173@zzrvtc.edu.cn

Abstract - With the widespread use of wireless communication systems, users' requirements for communication capabilities continue to increase, making base station equipment increasingly complex and channel estimation difficult. To address the problem of insufficient system capacity, research innovatively proposes using two sets of orthogonal waveforms to design a non-orthogonal multiple access scheme, combined with iterative interference cancellation technology and supporting detection channel estimation algorithms, to improve system capacity and spectral efficiency while optimizing channel estimation accuracy. The experiment shows that the system capacity of the non-orthogonal multiple access scheme proposed in the study is 4.5 bps/Hz, which is higher than the benchmark scheme and has an error rate of 10^{-5}. When the number of users is 16 and 32, the accuracy of the proposed channel estimation scheme is higher than that of the conventional orthogonal matching tracking method. The detection algorithm only supports NMSE values between 10^{-1}-10^{0} when the SNR value is 0, and between 1^{0-2}-10^{-1} when the SNR value is 3, achieving high accuracy values. The experimental results demonstrate that the proposed scheme can significantly improve system capacity and spectral efficiency, optimize channel estimation accuracy, and provide an efficient technical path for intelligent signal processing.

Keywords: Intelligent signal processing, Channel estimation, Channel scheme optimization, Wireless communication system, Non-orthogonal multiple access.

1. Introduction

With the rapid development of technology, signal processing plays an increasingly important role in many fields. Intelligent signal processing, as a crucial branch of signal processing, has been broadly utilized in radar, communication, sonar, biomedical and other fields due to its efficient and automated characteristics [1]. Compared to wired communication, wireless communication has merits such as good development prospects [2]. Channel scheme optimization is also a key link in intelligent signal processing, which directly affects the signal transmission's quality and efficiency [3]. Channel scheme optimization is a crucial step in ensuring that. In practical applications, the channel environment is often complex and variable, so it is necessary to optimize for different channel environments.

The channel scheme optimization includes optimization of channel models, channel coding, modulation and demodulation, etc. [4-5].
The channel scheme optimization can more accurately describe channel characteristics, providing better prediction and adaptability for signal transmission. The optimization of channel coding can improve the reliability and efficiency of signal transmission and reduce the error rate. The optimization of modulation and demodulation can better adapt to different channel conditions and improve the quality and stability of signal transmission [6]. Nevertheless, the growth of wireless communication cannot be separated from the support of wired communication. In practical applications, signals are often affected by various noises and interferences, leading to a decrease in signal quality. How to analyze and process these signals has become an urgent issue to be addressed. The research will focus on exploring the technical

https://doi.org/10.17683/ijomam/issue20.16

analysis and channel scheme optimization in intelligent signal processing, to provide useful references for research and application in related fields.

There are two main innovations of this study. The first point is to combine orthogonal frequency division multiple access (OFDMA) technology and code division multiple access (CDMA) multiple access technologies and design a non-orthogonal multiple access (NOMA) system, which not only retains the orthogonality of OFDMA in the frequency domain and the discriminative characteristics of CDMA in the code domain, but also further improves spectral efficiency through non-orthogonal resource sharing. The second point is to address the issue of interference between signal users in NOMA systems by proposing an iterative detection algorithm for serial interference cancellation, which improves the accuracy of signal detection through multiple iterative decisions.

This study is composed of four sections. Section 1 is a summary and explanation of the intelligent signal and channel scheme optimization. Section 2 is the implementation of the method raised in this study. Section 3 is the validation of the method raised in this study. Section 4 is a summary and outlook of the results of this study.

2. Related Works

In intelligent signal processing, purer signals can be extracted, providing a better foundation for subsequent feature extraction and pattern recognition. Pattern recognition technology is broadly applied in fields such as object detection, speech recognition, and biometric recognition. Bjrnson et al. bent and rotated homogeneous metal plates in various ways to explore the interaction with wireless radio frequency signals, allowing the incident wireless signals to undergo diffuse or mirror reflection in the desired manner. Using intelligent reflective surfaces, which are 2D arrays of metamaterials, the similar effect can also be realized electronically. By generating heterogeneous impedance changes on the surface, reflections of curved and rotating surfaces can be synthesized without any mechanical operation [7]. Mei W et al. considered a wireless network where multiple base stations use distributed IRSs to serve their respective downlink users. In particular, each IRS supports the transmission from its associated BS to the user through passive beamforming, leading to additional signals in the network. Thus, a new IRS/BS correlation issue has arisen that requires optimal balancing of the passive beamforming gains of all IRSs over various BS user communication links [8]. Chen J C considered the simultaneous optimization issue of access point transmission beamforming and intelligent reflector reflection beamforming in IRS assisted multi-user downlink systems. Owing to the complex combination of emission and reflection beamforming variables and the highly nonconvex constant mode restrictions, this joint optimization problems is nonconvex and hard. An alternative and modified framework was applied to decouple the joint optimization issue into two independent issues. Next, alternative optimization methods have been applied to optimize these issues individually. However, this alternative program may lead to performance degradation [9]. Ma Y et al. introduced a passive information transmission scheme in IRS-based multi-input, single-output systems. IRS offers additional auxiliary information to the user while increasing the communication from the main base station to the user. A joint beamforming and reflection optimization algorithm was developed to minimize the transmission power while guaranteeing the quality of the primary and secondary transmissions [10]. Yang H et al. studied a multi-user, multiple-input multiple-output (MIMO) wireless power transmission system supported by a reconfigurable smart surface. First, the study maximized the total received power of the users by optimizing the beamformer at the transmitter and the phase shift at the reconfigurable intelligent surface. Two sub-optimal solutions based on the alternate optimization were presented using the semi-definite relaxation technique and the successive convex approximation technique, respectively [11].

In practical applications, the channel environment is often complex and variable, so it is necessary to optimize for different channel environments. The optimization of channel schemes includes optimization of channel models, channel coding, modulation and demodulation, and other aspects. Saidutta Y M et al. proposed a learning scheme for source channel joint coding on simulated independent additive noise channels. By proving the upper bound relationship between the minimum loss function in rate distortion theory and the loss function of mutation autoencoder, a learning problem proof was proposed. When the dimension of the channel is smaller than that of the source, the encoding of two source samples may not necessarily be close to each other. This type of discontinuous projection must be accounted for by the use of multiple encoders and the selection of an encoder to encode samples on one side of the discontinuity [12]. Zhao X et al. studied the signal recovery properties of rectangular analog joint source channel coding with Doppler channels under high and medium/low signal-to-noise ratios (SNRs). With the geometric shape of rectangular simulation joint source channel coding in simulated sensing and Doppler effect systems, an analytical formula for mean square error performance was derived. A comprehensive list of all situations in the 3D geometric signal mapping curve was obtained. As a result, the theoretical formula for medium/low SNR situations was calculated. The evaluation result indicated that there were optimal parameters in high and medium/low-SNR rectangular AJSCC that could minimize signal recovery MSE of simulated sensors and Doppler effect systems [13]. Chen Q et al. put forward a dual original low density parity check codes JSCC scheme. A joint original image external information transformation algorithm was proposed to analyze the decoding threshold of low-density parity check codes with dual original images on non-standard encoding channels. Taking into account of the influence of source redundancy, the design of a low-density parity check structure with dual original graphs was analyzed, and new design principles were proposed [14]. Chang S H et al. used parameter methods to solve this nonlinear optimization issue in MIMO systems. Study used the parameter methods and derived some related attributes, and proposed an efficient optimization method using these attributes. In this method, the joint allocation of channel encoding and spatiotemporal encoding to data packets could be promoted. Thus, the designed method's computational complexity increased with the amount of data packets, and numerical analysis indicated that the designed method greatly increased the peak SNR of the traditional rate-based optimal solutions in MIMO systems [15]. Kochman Y addressed the classic source channel joint coding issue. The outcomes expressed that for uploading i.i.d uniform bits on a binary symmetric channel, if the bandwidth expansion ratio was greater than 1, the minimum achievable distortion bit error rate (BER) was at least higher than the asymptotic value of Omega (n (-1/2)) [16].

NOMA is a multi-user access technology that improves spectral efficiency through non-orthogonal resource sharing, and its performance is highly dependent on the accuracy of channel estimation. With the increasing demand for large-scale connectivity in 5G and 6G communication, the combination of NOMA and advanced channel estimation technology has become a research focus. Ahmad M et al. proposed a 6G network based on wavelet orthogonal frequency division multiple (OFDM) for NOMA combined with massive MIMO system, which can improve performance through wavelets. The results demonstrated that the proposed system outperformed the NOMA system based on fast Fourier transform (FFT) [17]. Salari A et al. proposed an uplink NOMA joint channel estimation and signal detection method based on unsupervised machine learning using Gaussian mixture model, and obtained the theoretical limit of the symbol error rate performance of the proposed method. The experimental results confirmed the effectiveness of the proposed method [18]. Kim D et al. proposed an Internet of Things (IoT) sub-channel and power allocation algorithm using downlink multi-carrier NOMA to support large-scale connectivity of IoT users.

The simulation results showed that compared with existing schemes, the proposed scheme had excellent overall rate and interrupt performance [19]. Ahmad M et al. stated that due to the freedom of non-orthogonality, NOMA leads orthogonal multiple access in terms of capacity and huge connectivity, but for MIMO systems, the capacity comparison between NOMA and orthogonal multiple access is very different [20]. It can be seen that Ahmad M et al.'s research mainly focuses on the combination of wavelet OFDM and NOMA, Salari A et al.'s research focuses on the application of unsupervised machine learning in NOMA, and Kim D et al.'s research focuses on sub-channels and power allocation algorithms in the IoT. This study combines OFDMA and CDMA to design an NOMA scheme, which achieves efficient transmission of multi-user access and signals, improves spectrum utilization and system capacity. In addition, this study uses an iterative method of serial interference cancellation to detect the NOMA scheme. Through multi-technology fusion, it can effectively eliminate interference between users and improve the accuracy of signal detection. In contrast, Ahmad M et al.'s research, although also involving the combination of NOMA and massive MIMO, lacks innovation in detection algorithms.

In summary, this study demonstrates unique innovation in intelligent signal processing and channel scheme optimization. Compared with existing research, this study not only combines OFDMA and CDMA to design an NOMA scheme, achieving efficient multi-user access and signal transmission, improving spectrum utilization and system capacity, but also adopts an iterative method of serial interference cancellation in the detection algorithm, effectively eliminating interference between users. On the other hand, Ahmad M et al.'s research mainly focused on the combination of wavelet OFDM and NOMA, which improved system performance, but relatively lacked innovation in the fusion of multiple access technologies and detection algorithms. Salari A et al.'s research mainly focused on the application of unsupervised machine learning in NOMA, while Kim D et al.'s research mainly addressed the connectivity needs of IoT users, and had relatively insufficient breadth and depth of technology integration compared to this study. The alternating optimization framework proposed by Chen J C et al. required multiple iterative optimizations and high computational complexity when solving the beamforming optimization problem of IRS assisted systems. Overall, this study has demonstrated unique innovative value in the integration of multiple access technologies, innovative detection algorithms, and improved channel estimation accuracy, providing new technical ideas and solutions for the field of intelligent signal processing.

2. Design of NOMA Scheme with OFDMA and CDMA and Model Selection for MIMO System

With the speed growth of wireless communication technology, multiple access and signal processing technologies are critical in communication systems. Building upon OFDMA and CDMA technologies, NOMA schemes have demonstrated unique advantages in using spectrum efficiently. In MIMO systems, model selection is equally crucial as it directly affects the quality and stability of signal transmission.

2.1 Design of NOMA Scheme with OFDMA and CDMA

With the advancement of 5G mobile communication networks, NOMA technology has received widespread attention.

Physical layer architecture of 5G cellular networks is based on large MIMO, waveforms, and mmWave technologies, while multiple access is central to wireless transmissions [21]. An NOMA system is proposed in the study, and on this basis, a serial interference cancellation iterative method is used to detect it. OFDMA has become the fundamental multiple access solution for 4G cellular systems, and has also been applied to mobile broadband services in 5G. Research has replaced the time dimension with the frequency dimension [22-23]. To provide a deeper explanation of the NOMA mechanism designed in this section, it is assumed that the OFDMA system has carriers and each carrier is assigned to different users without losing generality. The OFDMA system consists of multiple users, and each user in each OFDM symbol is assigned an orthogonal radiation modulation (QAM) symbol [24]. Figure 1 denotes the schematic diagram of the transmitter.

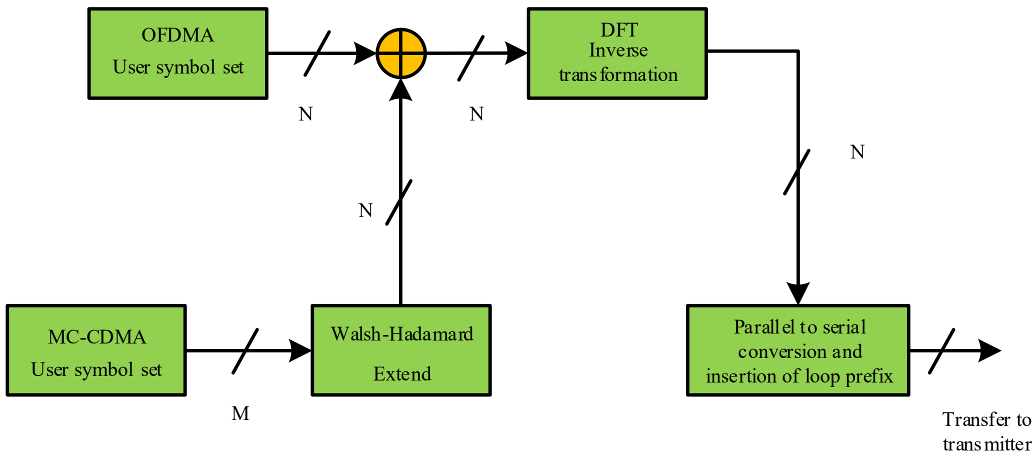

Figure 1: Principal diagram of using NOMA technology transmitter

In Figure 1, the OFDMA user module outputs an N dimensional QAM symbol vector, while the multi carrier-code division multiple access (MC-CDMA) user module is an M dimensional symbol vector $\{b_m\}, m\hat{I}[1,M]$. The Walsh-Hadamard extension extends the MC-CDMA symbol onto N carriers and outputs an N dimensional vector that is added to the OFDMA symbol vector. The signal block is transmitted to a N point discrete Fourier transform (DFT) inverse processing processor, and a cycle prefix (CP) is inserted between consecutive DFT blocks. In this design, the design scheme is summarized into the following steps: First is to set $N+M$ users, use the OFDMA orthogonal set system as the first set of OFDMA signal sets, and output N dimensional QAM symbol vectors from the first set of OFDMA signal sets $\{a_n\}, n\in[1,N]$. $\{b_m\}, m\in[1,M]$ is used as the second signal set to accommodate M users. The transmission signal x_n is obtained, as shown in formula 1.

$$x_n = a_n + \frac{1}{\sqrt{N}}\sum_{m=1}^{M} Wb_m \tag{1}$$

In formula (1), W represents the Walsh Hadamard sequence. A multiple access system based on multi-carriers is proposed, which uses multi-carriers to receive multiple carriers and superimposes them with multiple carriers to obtain an N dimensional vector. The second step is to iteratively determine the serial interference cancellation of the symbols of OFDMA signal and MC-CDMA signal. The received signal is $x_n+\varepsilon$, where ε represents additional noise. $x_n+\varepsilon$ is converted to the frequency domain through N

point DFT and undergoes the first iteration decision on $\{a_n\}, n \in [1, N]$ through a threshold detector to obtain the symbol decision value $\{\hat{a}_n\}, n \in [1, N]$. The sign decision value is subtracted from the operator y_n output by DFT, and the first iteration decision is made on $\{b_m\}, m \in [1, M]$ through a threshold detector, resulting in decision $\{\hat{b}_m\}, m \in [1, M]$. $\{\hat{b}_m\}, m \in [1, M]$ is subtracted from $x_n + \varepsilon$ and a threshold detector is used to make a second decision on $\{a_n\}, n \in [1, N]$ to obtain the symbol decision value. Finally, the symbol decision value of the second $\{a_n\}, n \in [1, N]$ is subtracted from $x_n + \varepsilon$, and the obtained signal is passed through a Walsh Hadamard de spreader.

Then, it continues to pass through a threshold detector for the second symbol decision value of $\{b_m\}, m \in [1, M]$ to obtain the symbol decision value of the second $\{b_m\}, m \in [1, M]$.

The multiple iterations of decision-making are repeated. The complexity analysis is shown in Table 1.

Table. 1 Complexity analysis

Technology	Time complexity	Space complexity	Description
OFDMA	O(N log N)	O(N)	The time complexity of each transformation is O (N log N), where N is the number of subcarriers
MC-CDMA	O(N log N)	O(N)	Spread spectrum and multi-carrier modulation are required, and the spread spectrum process requires the generation and processing of a large number of spreading codes
Serial interference cancellation	O(M)	O(M)	It is necessary to perform user by user detection and interference cancellation on the received signal, where M is the number of users

2.2 Model Evolution of Millimeter Wave Large-scale MIMO Systems

The millimeter wave MIMO system model has undergone a transformation from a pure digital model, a pure analog model to a combination of digital and analog models. The initial model is a pure digital model, as shown in Figure 2.

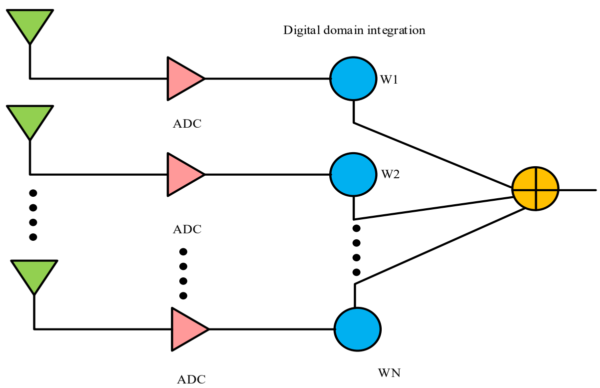

Figure 2: MMW large-scale MIMO structure

In Figure 2, pure digital beamforming technology is used to achieve a millimeter wave large-scale MIMO system, which has high spectrum utilization, high spatial resolution, strong anti-interference ability, high reliability, and flexible beamforming.

However, this method requires more transmission frequency links and is costly. A pure simulation model is used to reduce costs, and its MIMO structure is shown in Figure 3.

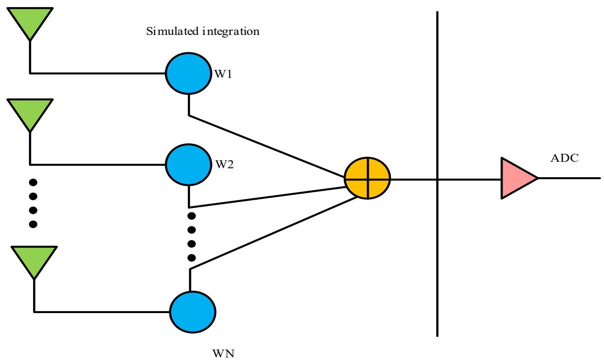

Figure 3: Millimeter-wave large-scale MIMO structure with purely simulated beam assignments

In Figure 3, this method only requires one analog-to-digital converter (ADC), which is low-cost and widely applicable in 60 GHz wireless communication. However, due to various factors, the application prospects of analog digital hybrid mode are better. In hybrid mode, the number of radio frequency links is less than the number of antennas. The hybrid array structure of antenna sharing is shown in Figure 4.

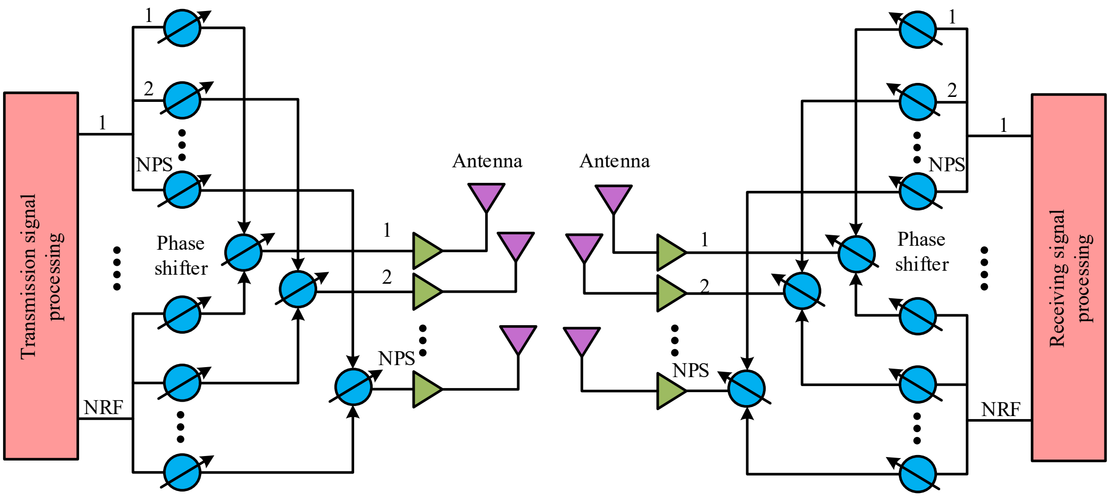

Figure 4: Hybrid array structure shared by the antennas

In Figure 4, it is a mixed array for antennas. The antennas in this hybrid array structure share the same antenna, which can greatly reduce hardware costs, save hardware resources, and reduce the size of the antenna array. However, this method also has some shortcomings. Firstly, due to antenna sharing, the multiplexing performance of the system is constrained. Secondly, due to factors such as channel estimation and hardware overhead, it is difficult to ensure sufficient orthogonality in the real beamforming domain.

Finally, in point-to-point user applications, due to the fact that antennas and amplifiers share multiple data streams, the central node cannot allocate power and gain control to multiple users, thereby limiting its application scope. The antenna of the hybrid array configuration is not a shared hybrid array, as shown in Figure 5.

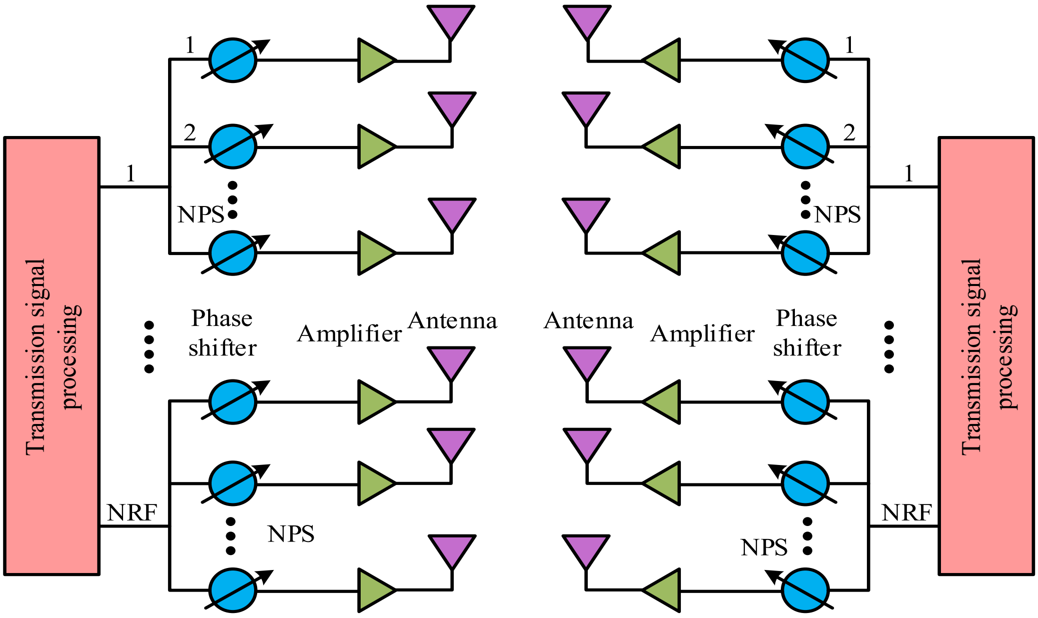

Figure 5: Combined array configuration of the antenna non-shared hybrid array

In Figure 5, a hybrid array with shared antennas is presented. Although this mode promotes the total volume and hardware cost of the system, it is more elastic, and in practical applications, its spatial freedom is much higher than that of hybrid arrays with shared antennas. In point-to-point user applications, due to the use of independent antennas and power amplifiers, the central node can achieve power allocation and gain control among multiple users, thereby expanding the applicability of non shared hybrid arrays. In the theory of compressive sensing, the mathematical representation of the compressive sensing model is shown in formula (2).

$$y = \Phi x = \Phi \Psi s = \theta s \tag{2}$$

In formula (2), x represents sparse signal, y represents observed communication signal, and the expression of θ is shown in formula (3).

$$\theta = \Phi\Psi \tag{3}$$

In formula (3), the concise model above has three key components of perception theory, namely the suitable transformation matrix Ψ, which is used to convert the initial ordinary signal into a sparse signal. Signal Φ is compressed. How to effectively construct high-dimensional x or s from low-dimensional observation communication signal y using effective recovery algorithms. The research assumes that a typical time-division duplex millimeter wave large-scale MIMO system is based on an actual lens 3D MIMO, as shown in Figure 6.

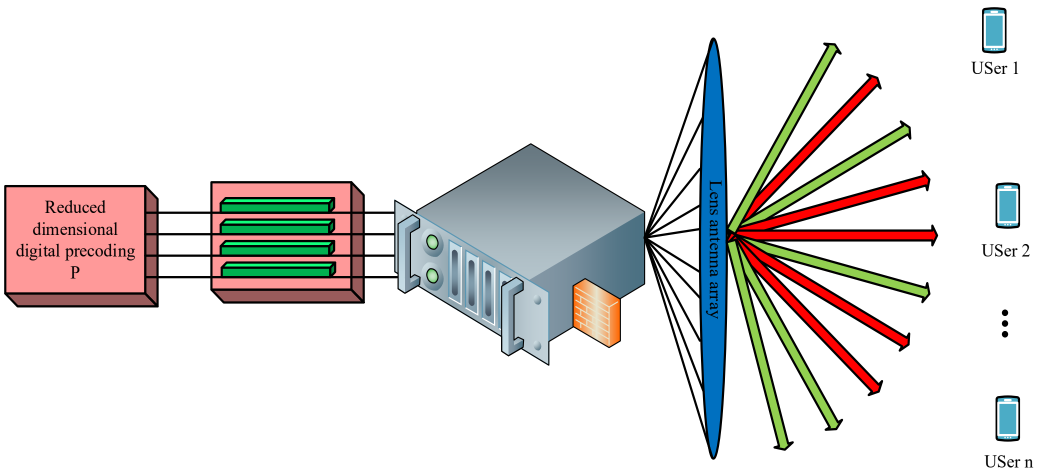

Figure 6: Lens-based 3 D MIMO sketch map

In Figure 6, mathematically speaking, this lens antenna array is an N × N spatial DFT matrix, as expressed in formula (4).

$$U = [a(i/N_1, j/N_2)]^H_{i\in L(N_1), f\in L(N_2)} \tag{4}$$

In formula (4), $i \in L(N_1)$ and $f \in L(N_2)$ denote predefined spatial azimuth and elevation angles, respectively. The MIMO system with 3D lenses is shown in formula (5).

$$\tilde{y}^{DL} = H^T U^T Ps + n \tag{5}$$

In formula (5), $\tilde{y}^{DL}$ means the received downlink signal vector, and $\tilde{H}^T = (UH)^T$ denotes the downlink channel matrix. Because of the limited amount of effective alignment paths in millimeter wave communication, using the adaptive selection network shown in Figure 6, fewer advantageous beams can be selected. The matrix of uplink signals $\tilde{y}^{UL}_m$ received at the base station is shown in formula (6).

$$\tilde{y}^{UL}_m = UH\Psi_m + N_m \tag{6}$$

In formula (6), Ψ_m represents the m-th block pilot matrix. N_m is the noise matrix of $N \times K$ in m blocks sampled in the baseband of the radio frequency link, and has uplink noise power.

The R_m of $K \times K$ sampled by the radio frequency link is shown in formula (7).

$$R_m = W_m \tilde{Y}^H_m \tag{7}$$

The measurement matrix z_m of the beam channel is shown in formula (8).

$$z_m = R_m \Psi^H_m = W_m \tilde{H} + N^{eff}_m \tag{8}$$

In formula (8), Ψ^H_m represents the pilot matrix, N^{eff}_m is the effective noise matrix without loss of generality and $\tilde{H}$ represents the beam channel. This scheme considers the beamspace channel estimation issue of the k th user, and the measurement vector $\bar{z}_k$ after pilot transmission is shown in formula (9).

$$\bar{z}_k = \begin{bmatrix} z_{1,K} \\ \dots \\ z_{M,K} \end{bmatrix} = \begin{bmatrix} W_1 \\ \dots \\ W_M \end{bmatrix} \bar{h}_k + \begin{bmatrix} n^{eff}_{1,K} \\ \dots \\ n^{eff}_{M,K} \end{bmatrix} \tag{9}$$

In formula (9), $\bar{h}_k$ represents the k-th user of the beam space channel. The supporting detection channel estimation algorithm first detects the strongest element index p in $\tilde{c}_l$, and calculates the strongest and column indices as $i^* = \frac{p}{N_2}$ and

$j^* = p - N_2(i^* - 1)$. Subsequently, the algorithm adaptively detects the support level of $\tilde{c}_l$. The classic least squares (LS) algorithm can estimate non-zero edge element 1 as shown in formula (10).

$$M_1 = \left| \tilde{c}_l^e(i^*, j^* - V_2/2) \right| \tag{10}$$

The classic LS algorithm can estimate non-zero edge elements 2, as shown in formula (11).

$$M_2 = \left| \tilde{c}_l^e(i^*, j^* + V_2/2 - 1) \right| \tag{11}$$

The classic LS algorithm can estimate non-zero edge elements 3, as shown in formula (12).

$$M_3 = \left| \tilde{c}_l^e(i^* - V_1/2, j^*) \right| \tag{12}$$

The classic LS algorithm can estimate non-zero edge elements 4 as shown in formula (13).

$$M_1 = \left| \tilde{c}_l^e(i^* + V_1/2, j^*) \right| \tag{13}$$

If $\min(M_1, M_2) < \min(M_3, M_4)$, the power diffusion in the vertical direction of the spatial channel is more severe, otherwise the power diffusion in the horizontal direction is more severe. Then, the influence of channel components is removed using formula (14).

$$\bar{z}_k^{l+1} = \bar{z}_k^l - \bar{W}^H \tilde{c}_l^e \tag{14}$$

Keep repeating until all channel components are processed. Finally, the overall support of $\bar{h}_k$ is obtained, and the LS algorithm is used to estimate the beam space channel of user k based on the overall support.

3. Simulation Analysis of NOMA and Support Detection Channel Estimation Algorithms based on OFDMA and CDMA

Based on the simulation software Matlab, the NOMA algorithm and the support detection channel estimation algorithm were simulated and explored, and their performance was explored to explore the role of iterative reweighting operation in avoiding quantization errors, to achieve super-resolution channel estimation.

3.1 Analysis and Comparison of NOMA Simulation Experiments based on OFDMA and CDMA

The proposed NOMA algorithm was simulated using Matlab. Simulation was conducted on additive Gaussian white noise (AWGN) channels. 16QAM modulation was used for OFDMA users, and QPSK was used for MC-CDMA users. In the first group of simulation, the amount of MC-CDMA users was 4, and the BERs of OFDMA users and MC-CDMA (N =64, M =4) are shown in Figure 7.

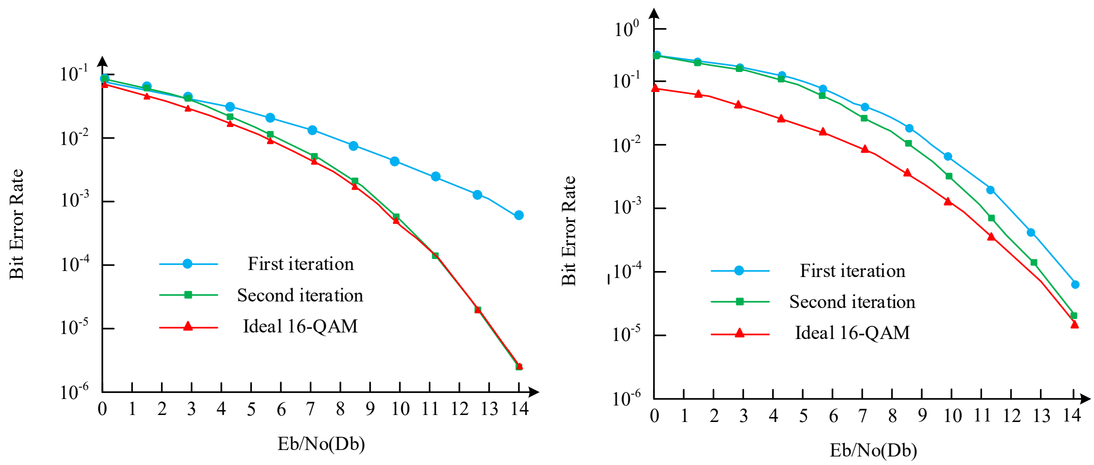

(a) OFDMA User (N=64,M=4) Bit Error Rate

(b) MC-CDMA User (N=64,M=4) Bit Error Rate

Figure 7: OFDMA user (N =64, M =4) BER

In Figure 7, Figure 7 (a) represents the performance of OFDMA users at M =4, and Figure 7 (b) represents the performance of MC-CDMA users at M =4. In Figure 7 (a), at the first iteration, the BER curve of user OFDMA was greatly various from the theoretical curve of 16-QAM. However, the second iteration significantly improved performance, with detection results very close to the theoretical BER curve, and the BER after the second iteration was below 10^{-3}. The preliminary reason for the error may be interference from MC-CDMA users. In Figure 7 (b), there are several different performance characteristics in the MC-CDMA system. The BER of the first iteration was within 1dB, and the dislocation rate was within 10^{-4}, which was basically consistent with the dislocation rate curve under QPSK modulation. After two iterations, the performance of the system greatly improved, and the BER curve was basically consistent with the theoretical BER curve of QPSK, with a dislocation rate below 10^{-5}. The research results showed that when (N =64, M =4), this method only required two iterations to effectively eliminate interference between OFDMA users and MC-CDMA users. In the second group of simulation, the amount of MC-CDMA users was 8, and the BERs of OFDMA and MC-CDMA users (N =64, M =8) are shown in Figure 8.

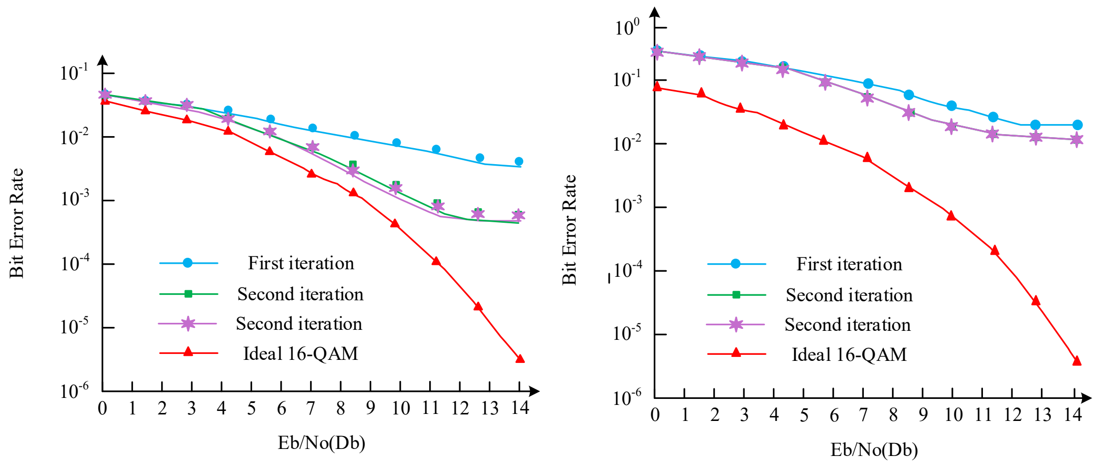

Figure 8: OFDMA user (N =64, M =8) BER

In Figure 8, Figure 8 (a) represents the outcomes for OFDMA users with M =8. Figure 8 (b) represents the corresponding results for MC-CDMA users with M =8. In Figure 8 (a), at the first iteration, the BER curve decreased over time. The BER improved in the second iteration, but it was evident from the curve that the BER approached 10^{-3}. The third loop only had a small improvement. In Figure 8 (b), in the first cycle, the BER curve was stationary, while in the second cycle, there was only a small improvement. In the third loop, the BER value was very small, and the BER value was greater than 10^{-2}. This simulation result showed that if an iterative receiver was used for decision-making, the number of MC-CDMA users needed to be controlled below the $\sqrt{N}$ range to avoid excessive error rates. The study used the traditional total access communications system (TACS) system, GSM system, and NOMA scheme as benchmarks. The system capacity and BER of the proposed NOMA scheme were further compared with these three benchmarks, as shown in Table 2.

Table. 2 Comparison of system capacity and BER for four solutions

Scheme	Technology	System capacity (bps/Hz)	BER
TACS system	FDMA	0.1	10^{-3}
GSM system	TDMA	1.5	10^{-5}
NOMA scheme	NOMA	3.0	10^{-4}
Proposed NOMA scheme	OFDMA and MC-CDMA	4.5	10^{-5}

From Table 2, the system capacity of the NOMA scheme proposed by the research was 4.5 bps/Hz, which was higher than the benchmark scheme and had a lower BER of 10^{-5}. In summary, a multi-access method based on OFDM and MC-CDMA was proposed by combining the most popular OFDMA and MC-CDMA in 5G. The simulation experiment results showed that the raised scheme could promote the system capacity without reducing system effectiveness.

3.2 Simulation Analysis of Support Detection Channel Estimation Algorithms and Performance Analysis of Channel Estimation Schemes

A 16 radio frequency link equipped at the base station was researched, with a lens N of 1024 at a horizontal position of 32 and a vertical position of 32, to serve K users simultaneously. When the time slot for pilot transmission was 256, for the support detection scheme $V_1 = V_2 = 8$, and for the channel estimation scheme based on orthogonal matching tracking, assuming the dilution level of the three-dimensional beam space channel was 192, the performance comparison of normalized mean square error (NMSE) using the support detection scheme and conventional orthogonal matching tracking method is shown in Figure 9.

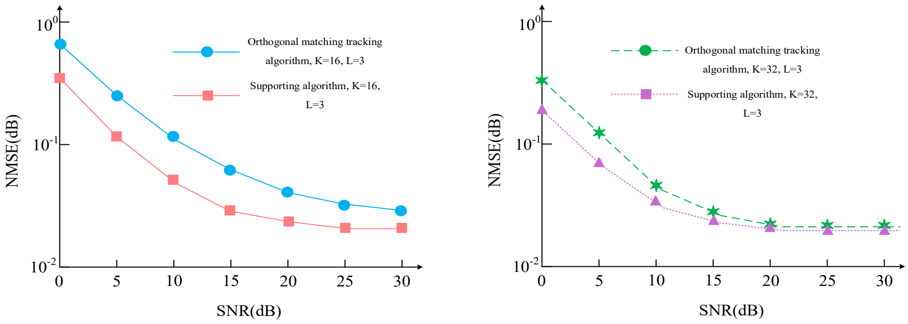

(a) Comparison of normalized mean square error performance between orthogonal matching tracking algorithm and professional title detection algorithm at K=16, L=3

(b) Comparison of normalized mean square error performance between orthogonal matching tracking algorithm and professional title detection algorithm at K=32, L=3

Figure 9: Comparison of NMSE performance between orthogonal matching tracking algorithm and support detection algorithm

In Figure 9, compared with the channel estimation scheme based on orthogonal matching tracking algorithm, the channel estimation scheme based on support detection had a significant improvement in accuracy, regardless of the number of users $K = 16$ or $K = 32$. The quantitative comparison of the performance of NMSE using support detection scheme and conventional orthogonal matching tracking method is shown in Table 3.

Table. 3 Quantified numerical values to support the detection scheme and the performance of NMSE using conventional orthogonal matching tracking methods

Algorithm type/ variable	K Value	L Value	SNR(dB)	NMSE(dB)
Orthogonal matching tracking algorithm	16	3	0	10-1-100
			5	10-1-100
			10	10-1-100
			15	10-2-10-1
			20	10-2-10-1
			25	10-2-10-1
			30	10-2-10-1
Supporting algorithm	16	3	0	10-1-100
			5	10-1-100
			10	10-2-10-1
			15	10-2-10-1
			20	10-2-10-1
			25	10-2-10-1
			30	10-2-10-1
Orthogonal matching tracking algorithm	32	3	0	10-1-100
			5	10-1-100
			10	10-2-10-1
			15	10-2-10-1
			20	10-2-10-1
			25	10-2-10-1
			30	10-2-10-1
Supporting algorithm	32	3	0	10-1-100
			5	10-2-10-1
			10	10-2-10-1
			15	10-2-10-1
			20	10-2-10-1
			25	10-2-10-1
			30	10-2-10-1

In Table 3, the channel estimation scheme based on support detection significantly improved accuracy at $K=16$ and the number of users $K=32$. When the SNR value was between 0-30, the NMSE value was mostly between 10^{-2}-10^{-1}, and when the SNR value was 0, the NMSE value was between 10^{-1}-10^{0}, achieving high accuracy. This may be because the channel estimation scheme based on support detection selects the atoms most relevant to the current residual in each iteration step, gradually constructing a sparse representation of the signal, which can effectively suppress the influence of noise, thus performing well in SNR environment and having high estimation accuracy. The channel estimation scheme based on orthogonal matching tracking algorithm had a slightly higher computational complexity, optimizing all selected dictionary elements in each iteration. Therefore, it may be greatly affected by noise in low SNR environments, leading to a decrease in estimation accuracy. The performance of the channel estimation scheme was validated using Matlab, and the situation of using hybrid precoding technology to reduce the amount of RF links was studied. The parameters were set to $N_T=10$, $N_{RF}=4$, $d=\lambda/2$, $N_X=Q=24$. The performance of orthogonal matching tracking algorithm and second-order block weighted l_1-Minimization algorithm was compared with support detection algorithm. The outcomes are indicated in Figure 10.

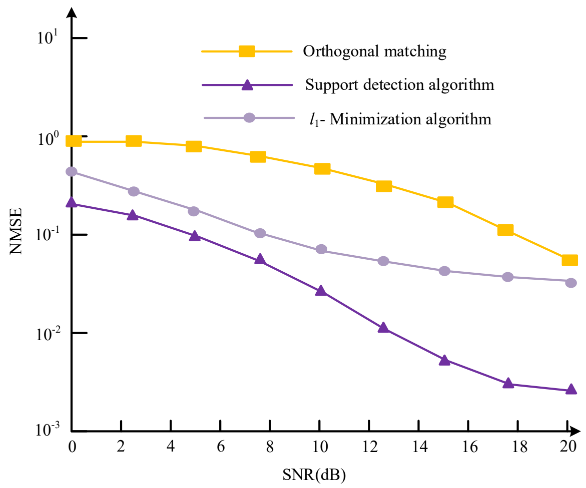

Figure 10: NMSE performance of several channel estimation schemes

In Figure 10, the NMSE effectiveness of three channel estimation schemes is shown, among which the channel estimation scheme based on support detection performed the best. Due to the quantization error caused by parameter discretization in the supporting detection scheme, the iterative reweighting operation studied effectively avoided this problem, thus achieving super-resolution channel estimation. The range of NMSE values for the three channel estimation schemes is denoted in Table 4.

Table. 4 The range of NMSE values for three channel estimation schemes

SNR (dB)/Channel estimation scheme	Support detection algorithm (NMSE)	l1-Minimization algorithm (NMSE)	Orthogonal matching (NMSE)
0	10^{-1}-10^{0}	10^{-1}-10^{0}	10^{-1}
2	10^{-1}-10^{0}	10^{-1}-10^{0}	10^{-1}
4	10^{-1}	10^{-1}-10^{0}	10^{-1}-10^{0}
6	10^{-2}-10^{-1}	10^{-1}-10^{0}	10^{-1}-10^{0}
8	10^{-2}-10^{-1}	10^{-2}-10^{-1}	10^{-1}-10^{0}
10	10^{-2}-10^{-1}	10^{-2}-10^{-1}	10^{-1}-10^{0}
12	10^{-2}-10^{-1}	10^{-2}-10^{-1}	10^{-1}-10^{0}
14	10^{-2}-10^{-1}	10^{-2}-10^{-1}	10^{-1}-10^{0}
16	10^{-2}-10^{-1}	10^{-2}-10^{-1}	10^{-1}-10^{0}
18	10^{-2}-10^{-1}	10^{-2}-10^{-1}	10^{-2}-10^{-1}
20	10^{-2}-10^{-1}	10^{-2}-10^{-1}	10^{-2}-10^{-1}

Table 4 shows the range of NMSE values for three different channel estimation schemes under different SNR conditions. Under low SNR conditions, the NMSE values of all algorithms were roughly between 10^{-1} and 10^{0}, reflecting that the accuracy of channel estimation was lower when the noise level was high. With the increase of SNR, the performance of support detection algorithm and l_1-Minimization algorithm gradually improved, and the NMSE value dropped to between 10^{-2} and 10^{-1}. In contrast, the overall NMSE value of orthogonal matching is higher. To further verify the superiority of the proposed NOMA scheme, Matlab 2023a was used to simulate and analyze static Rayleigh fading channels and high-speed mobile scenarios. In high-speed mobile scenarios, the user speed was 120 km/h, the Doppler frequency shift was 500 Hz, the number of OFDMA subcarriers was 64, the number of users was 64, and the SNR was 20 dB.

The proposed scheme was compared with four mainstream NOMA schemes: traditional OFDMA, Sparse Code Multiple Access (SCMA), Power Domain NOMA (PD-NOMA), and Multi User Shared Access (MUSA).

The performance comparison results of multiple access technologies for the five schemes are shown in Table 5.

Table. 5 Comparison of Multiple Access Technology Performance among Five Solutions

Scheme	System capacity (bps/Hz)	BER (static state)	BER (mobility)	Calculate time complexity
OFDMA	2.3	10^{-3}	10^{-2}	O(N log N)
SCMA	5.1	10^{-5}	10^{-4}	O(N log N)
PD-NOMA	4.8	10^{-4}	10^{-3}	$O(M^2)$
MUSA	5.4	10^{-5}	10^{-4}	O(M log M)
Proposed NOMA	6.2	10^{-6}	10^{-5}	O(M)

From Table 5, the BER of the proposed NOMA scheme in static and high-speed mobile scenarios was 10^{-6} and 10^{-5}, respectively, both lower than the other four mainstream NOMA schemes, indicating higher data transmission quality. Moreover, the NOMA scheme had the highest system capacity, at 6.2 bps/Hz. Next was MUSA, with a system capacity of 5.4 bps/Hz. In addition, the proposed solution had a time complexity of O (M), significantly lower than the O (M^2) of PD-NOMA, making it more suitable for real-time processing. This is because the NOMA scheme proposed by the research adopted a serial interference cancellation iterative detection algorithm at the receiving end, which can effectively reduce inter user interference, improve signal detection accuracy, and thus improve the system error rate. In addition, by combining OFDMA and CDMA with NOMA, more dimensional resource allocation and interference management strategies could be created, which helps to improve system capacity and flexibility, and enhance multi scenario adaptability. The results indicated that the proposed scheme surpassed existing technologies in key performance indicators such as system capacity, BER, and computational complexity, providing an efficient and flexible multiple access scheme for the future development of communication systems. It has significant scientific innovation value and broad industrial application prospects.

4. Conclusions

With the increasing number of terminals connected to base stations, the communication needs of users are also increasing, which leads to the increasing complexity of base station equipment and the difficulty of channel estimation. This project aims to address the limited channel capacity in current wireless communication networks and proposes the use of two sets of orthogonal signals, combined with iterative interference cancellation methods, to conduct research on non orthogonal multiple access mechanisms. Through simulation analysis of the proposed scheme, the findings denoted that when the number of users in two groups reached a certain proportion, the system capacity could be improved without reducing performance, which is an expansion of orthogonal multiple access technology. In the performance comparison experiment using support detection scheme and conventional orthogonal matching tracking method for NMSE, the channel estimation scheme based on support detection showed significant improvement in accuracy when $K = 16$ and the number of users were $K = 32$. When the SNR value was between 0-30, the NMSE value was mostly between 10^{-2}-10^{-1}, and the support detection algorithm only achieved high accuracy when the SNR value was 0, the NMSE value was between 10^{-1}-10^{0}. In summary, the NOMA scheme proposed by the research combines the advantages of OFDMA and CDMA, and adopts an iterative detection algorithm of serial interference cancellation, which can improve the system capacity without significantly reducing system performance. In practical applications, this means that a high-quality communication service can be provided to more users within the same spectrum bandwidth and base station coverage range, which is of great significance for addressing high user density and high traffic demand scenarios in densely populated areas. However, millimeter wave massive MIMO systems and NOMA technology require high hardware equipment, and the procurement, installation, and maintenance costs of hardware equipment may become an important factor limiting the widespread application of this solution. Therefore, in future research, further development of low-cost and high-performance millimeter wave massive MIMO hardware devices should be carried out.

Fundings

The research is supported by Mobile robot positioning system based on optical flow tracking and feature point matching，Key scientific research projects of colleges and universities in Henan Province in 2024，NO.24B510015.

Reference

[1] Zhang L, Yang X, Liu H, Zhang H, Cheng J. Efficient Residual Shrinkage CNN Denoiser Design for Intelligent Signal Processing: Modulation Recognition, Detection, and Decoding. IEEE Journal on Selected Areas in Communications, 2022, 40(1):97-111.

[2] Zhang Y, Jiang L. A Novel Demultiplexing Scheme for Vortex Beams in Radio Communication Systems. IEEE Transactions on Vehicular Technology, 2021, 70(7):7243-7248.

[3] Kamal M A S, Hayakawa T, Imura J I. Development and Evaluation of an Adaptive Traffic Signal Control Scheme Under a Mixed-Automated Traffic Scenario. IEEE Transactions on Intelligent Transportation Systems, 2020, 21(2):590-602.
[4] Jin S, Liu Y, Fagherazzi S, Mi H, Qiao G, Xu W, Sun C, Liu Y, Zhao B, Fichot C. River body extraction from sentinel-2A/B MSI images based on an adaptive multi-scale region growth method. Remote Sensing of Environment, 2021, 255(8):112297-112317.
[5] Liu W, Cao Y, Wang X, Li X. Continuous-variable quantum key distribution under strong channel polarization disturbance. Physical Review A, 2020, 102(3):32625-32631.
[6] Ammar A, Zhang Y D, Yujie G. Dual-Function Radar-Communications Using QAM-based Sidelobe Modulation. Digital Signal Processing, 2018, 82(11):166-174.
[7] Bjrnson E, Marcenaro L. Configuring an Intelligent Reflecting Surface for Wireless Communications: Highlights from the 2021 IEEE Signal Processing Cup student competition [SP Competitions]. IEEE Signal Processing Magazine, 2022, 39(1):126-131.
[8] Mei W, Zhang R. Performance Analysis and User Association Optimization for Wireless Network Aided by Multiple Intelligent Reflecting Surfaces.IEEE Transactions on Communications, 2021, 69(9):6296-6312.
[9] Chen J C. Machine Learning-Inspired Algorithmic Framework for Intelligent Reflecting Surface-Assisted Wireless Systems. IEEE Transactions on Vehicular Technology, 2021, 70(10):10671-10685.
[10] Ma Y, Liu R, Li M, Liu Q. Passive Information Transmission in Intelligent Reflecting Surface Aided MISO Systems. IEEE Communications Letters, 2020, 24(12):2951-2955.
[11] Yang H, Yuan X, Fang J, Liang Y. Reconfigurable Intelligent Surface Aided Constant-Envelope Wireless Power Transfer. IEEE Transactions on Signal Processing, 2021, 69(2):1347-1361.
[12] Saidutta Y M, Abdi A, Fekri F. Joint Source-Channel Coding Over Additive Noise Analog Channels Using Mixture of Variational Autoencoders. IEEE Journal on Selected Areas in Communications, 2021, 39(7):2000-2013.
[13] Zhao X, Sadhu V, Pompili D. Signal Recovery Performance Analysis in Wireless Sensing with Rectangular-Type Analog Joint Source-Channel Coding. IEEE transactions on wireless communications, 2023, 23(2):734-745.
[14] Chen Q, Wang L. Design and Analysis of Joint Source Channel Coding Schemes over Non-standard Coding Channels.IEEE Transactions on Vehicular Technology, 2020, 69(5):5369-5380.
[15] Chang S H, Shin M, Kim S H. Joint Source, Channel, and Space-Time Coding of Progressive Bitstream in MIMO Channels. IEEE Transactions on Communications, 2020, 68(4):2551-2565.
[16] Kochman Y, Ordentlich O, Polyanskiy Y. A Lower Bound on the Expected Distortion of Joint Source-Channel Coding. IEEE Transactions on Information Theory, 2020, 66(8):4722-4741.
[17] Ahmad M, Shin S Y. Massive MIMO NOMA with wavelet pulse shaping to minimize undesired channel interference. ICT Express, 2023, 9(4): 635-641.
[18] Salari A, Shirvanimoghaddam M, Shahab M B, Arablouei R, Johnson S. Design and analysis of clustering-based joint channel estimation and signal detection for NOMA. IEEE Transactions on Vehicular Technology, 2023, 73(2): 2093-2108.
[19] Kim D, Jung H, Lee I H, Niyato D. Novel Resource Allocation Algorithm for IoT Networks With Multi-Carrier NOMA. IEEE Internet of Things Journal, 2024, 11(18): 30354 - 30367.
[20] Ahmad M, Ramatryana I N A, Shin S Y. Noma and OMA comparison for multiple antenna technologies under high capacity constraints for 5G and beyond. 한국통신학회논문지, 2020, 45(11): 2004-2013.
[21] Zhang G, Gao Y, Luo H, Liu X, Sha N, Xu K. Security-Reliability Tradeoff for Joint Relay-User Pair and Friendly Jammer Selection with Channel Estimation Error in Internet-of-Things.I EICE Transactions on Communications, 2021, 104(6):686-695.
[22] Tan L, Kuang Z, Zhao L, Liu A. Energy-Efficient Joint Task Offloading and Resource Allocation in OFDMA-Based Collaborative Edge Computing. IEEE transactions on wireless communications, 2022, 21(3):1960-1972.
[23] Dube P, Walingo T. Performance analysis of an adaptive OFDMA-based CSMA/CA scheme on a wireless network. IET Communications, 2020, 14(19):3480-3489.
[24] Mokayed H., Quan, T Z, Alkhaled L, Sivakumar V. Real-time human detection and counting system using deep learning computer vision techniques. Artificial Intelligence and Applications. 2023, 1(4): 221-229.